SHORT-TERM SOLAR PRESSURE EFFECT AND GM UNCERTAINTY ON TDRS ORBITAL ACCURACY A STUDY OF THE INTERACTION OF MODELING ERROR WITH TRACKING AND ORBIT DETERMINATION

Bertrand T. Fang

EG&G Washington Analytical Services Center, Inc.

ABSTRACT

The interaction of modeling errors with the tracking and orbit determination of TDRS satellites is studied. For orbit determination instead of long-term orbit prediction and station-keeping, it is convenient to express TDRS orbital errors as radial, along-track and cross-track deviations from a nominally circular orbit. Simple analytical results are given for the perturbation of TDRS orbits as a result of GM uncertainty; as a result of changes in epochal elements; as a result of solar radiation uncertainty, with the TDRS modeled as a combination of a sun-pointing solar panel and an earth-pointing plate. Based on this simplified model, explanations are given for the following orbit determination error characteristics: inherent limits in orbital accuracy, the variation of solar pressure induced orbital error with time of the day of epoch, the insensitivity of range-rate orbits to GM error, and optimum bilateration baseline. The result should also shed some light on the general subject of the interaction of modeling error with orbit determination.

SHORT-TERM SOLAR PRESSURE EFFECT AND GM UNCERTAINTY ON TDRS ORBITAL ACCURACY - A STUDY OF THE INTERACTION OF MODELING ERROR WITH TRACKING AND ORBIT DETERMINATION*

Bertrand T. Fang
EG&G/Washington Analytical Services Center, Inc.
Riverdale, Maryland 20840

I. INTRODUCTION

It is known (Ref. 1,2) that uncertainties in GM and solar radiation pressure force are two major sources of error for the orbit determination accuracies of the geosynchronous Tracking and Data Relay Satellities (TDRS). The magnitudes of the resulting orbit errors depend on the configuration of tracking baseline and the time of the day chosen as epoch. These and other perplexing phenomena observed in the course of error analysis results from a complex interplay between modeling error induced orbit perturbations and compensations provided by tracking and orbital computations. The present study is undertaken to seek a better physical understanding of modeling error and its interaction with tracking and orbit determination. Analytical derivations are pursued, together with a digestion of available numerical results. Although the impetus of the present study concerns TDRS orbital accuracy, it is hoped the results will shed some light on the subject in general.

Sections II and III below give simple analytical results for the perturbation of TDRS orbits in the presence of solar radiation pressure and GM uncertainty. From these results, the inherent limit of orbit determination accuracy in the

*This investigation is supported by NASA Goddard Space Flight Center (GSFC). Additional details are contained in an EG&G/WASC report to GSFC.

presence of modeling errors is derived in Section IV. The information conveyed by range and range-rate measurements is studied. Based on the information content of measurements and the orbital perturbations resulting from modeling errors, certain idiosyncrasies in orbit determination errors and characteristics are explained.

II. SHORT-TERM SOLAR RADIATION PERTURBATION OF TDRS ORBITS

Perturbation of artificial satellites by solar radiation pressure has been studied extensively (Ref.3). However, with very few exceptions, these studies are mainly concerned with the long-term perturbations of the Keplerian elements of a spherical satellite, and with the shadow effect.

For the present purpose, the following model shall be adopted:

1. The unperturbed TDRS orbit is a circular orbit about a homogeneous spherical earth.

2. The sun-to-TDRS vector may be considered a constant in inertial space during the short period (several days) of interest.

3. The TDRS satellites may be modeled as the combination of a sun-pointing solar panel and an earth-pointing perfectly reflecting flat disk. Any shadowing by the earth or by part of the satellite itself is neglected.

The relative geometry of the TDRS, the Sun, and the unperturbed TDRS orbit is shown in Fig. 1. The equations of motion governing the "cross-track", "radial" and "along-track" perturbations

from a nominally circular orbit may be expressed in the following convenient forms (Ref. 4,5):

$$\ddot{z} + z = f_Z \qquad (1)$$

$$\delta\ddot{\rho} - 3\delta\rho - 2R\dot{\delta\theta} = f_\rho \qquad (2)$$

$$R\ddot{\delta\theta} + 2\dot{\delta\rho} = f_\theta \qquad (3)$$

where a superposed dot denotes differentiation with a normalized time τ, which represents the nominal angular position of TDRS. R is the nominal orbital radius of TDRS. The f's are components of the solar radiation force per unit TDRS mass. For our model f_Z is a small constant quantity. The cross-track perturbation as given by the solution of Eq. (1) represents small oscillations uncoupled to the other perturbations and shall not be considered further. Eq. (2) and (3) may be rearranged as

$$\delta\ddot{\rho} + \delta\rho = f_\rho + 2\int f_\theta d\tau \qquad (2a)$$

$$R\dot{\delta\theta} = -2\delta\rho + \int f_\theta d\tau. \qquad (3a)$$

which show that solar radiation force components at the orbital frequency, as well as any constant tangential component, will cause secular perturbations and are of primary importance. Eq. (3a), with the term $-2\delta\rho$ moved to the left-hand side of the equality sign, relates the tangential force to the change in orbital angular momentum.

Let us consider the Sun-pointing solar panel first. For this case one may write

$$f_\rho = f_{xy}\,\mathrm{Cos}(\phi-\tau)$$

$$f_\theta = f_{xy}\,\mathrm{Sin}(\phi-\tau)$$

where f_{xy} is the component of the solar radiation force on the solar panel in the TDRS orbital plane and $(\phi-\tau)$ is the angle between his force component and the TDRS orbital radius. It is straight-forward to show Eq. (2) and (3) admit the following general solution under these forces:

$$\begin{bmatrix} \delta\rho(\tau) \\ \dot{\delta\rho}(\tau) \\ R\delta\theta(\tau) \\ R\dot{\delta\theta}(\tau) \end{bmatrix} = [A] \begin{bmatrix} \delta\rho(0) \\ \dot{\delta\rho}(0) \\ R\delta\theta(0) \\ R\dot{\delta\theta}(0) \end{bmatrix} + f_{xy} ([B] + \tau[C]) \tag{4}$$

$$[A] = \begin{bmatrix} 4-3\cos\tau & \sin\tau & 0 & 2(1-\cos\tau) \\ 3\sin\tau & \cos\tau & 0 & 2\sin\tau \\ 6(\sin\tau-\tau) & 2(\cos\tau-1) & 1 & 4\sin\tau-3\tau \\ 6(\cos\tau-1) & -2\sin\tau & 0 & 4\cos\tau-3 \end{bmatrix} \tag{5}$$

$$[B] = \begin{bmatrix} \frac{3}{2}\sin\phi\sin\tau - 2\cos\phi(1-\cos\tau) \\ -\frac{1}{2}\cos\phi\sin\tau \\ -\cos\phi\sin\tau - 5\sin\phi - 5\sin(\tau-\phi) \\ 3\cos\phi - 3\cos\phi\cos\tau - 2\sin\phi\sin\tau \end{bmatrix} \tag{6}$$

$$[C] = \begin{bmatrix} \frac{3}{2}\sin(\tau-\phi) \\ \frac{3}{2}\cos(\tau-\phi) \\ 3\cos\phi + 3\cos(\tau-\phi) \\ -3\sin(\tau-\phi) \end{bmatrix} \tag{7}$$

Notice the first term on the right-hand side of Eq. (4) is the homogeneous solution which represents orbit perturbations resulting from changes in the initial conditions. The "state transition matrix" [A] is well-known, see for instance Ref. 6.

The solution as given in Eq. (7) indicates the more important effect of solar radiation is to cause a linearly diverging oscillatory (at the orbital rate) perturbation in radial and along-track motion. In addition, the perturbation in the along-track orbital position depends on the initial sun angel ϕ as illustrated in Figures 2 and 3. The least perturbation occurs when the sun vector is parallel to the satellite velocity vector in the beginning. The worst perturbation doubles that of the least perturbation and occurs when the sun is overhead or underfoot in the beginning. This dependence on initial sun angle may seem a bit perplexing. The explanation lies in that starting from the time the sun is overhead there is a duration of one-half orbit for the building-up of angular momentum. On the other hand, starting from the time when the sun is directly behind the satellite velocity vector there is only one-quarter of an orbit for the orbital angular momentum to build-up before the satellite turns around and is opposed by the solar radiation force. Similar situations occur when the sun is underfoot or directly opposed to the satellite velocity vector.

The non-homogeneous part of the above solution, represting perturbations of a sun-pointing or spherical satellite, in various equivalent forms, are well-known, although the dependence of the solution on initial sun angle has not been empasized.

For the earth-pointing part of TDRS, the solar radiation force may be expressed as

$$f_\rho = K|\cos(\phi-\tau)|\cos(\phi-\tau)$$

$$f_\theta = o,$$

the latter vanishes because this part of TDRS is modeled as a perfectly-reflecting disk. The term $|\cos(\tau-\phi)|$ represents the projected area which intercepts the incoming radiation. The absolute sign presents a minor complication and can be handled by the standard Fourier expansion technique. The particular solution of Eq (2) and (3) describing the perturbation of an earth-pointing perfectly-reflecting flat disk can then be written as

$$\delta\rho = \frac{4K}{3\pi}\tau\sin(\tau-\phi) - \frac{4K}{3\pi}\sin\phi\sin\tau + \frac{8K}{\pi}\left\{\frac{\cos 3(\tau-\phi)-\cos 3\phi}{(1-3^2)(1\cdot 3\cdot 5)} - \frac{\cos 5(\tau-\phi)-\cos 5\phi}{(1-5^2)(3\cdot 5\cdot 7)} + \ldots\right\} \quad (8)$$

$$R\delta\theta = \frac{8K}{3\pi}\left\{\tau\cos(\tau-\phi) - \sin\tau\cos\phi\right\} - \frac{16K}{\pi}\left\{\frac{\frac{1}{3}[\sin 3(\tau-\phi)+\sin 3\phi]-\cos 3\phi}{(1-3^2)(1\cdot 3\cdot 5)} - \right. \quad (9)$$

$$\left. - \frac{\frac{1}{5}[\sin 5(\tau-\phi)+\sin 5\phi]-\cos 5\phi}{(1-5^2)(3\cdot 5\cdot 7)} + \ldots\right\}$$

It is seen the primary perturbations are still diverging oscillations at the orbital rate. As compared with that of a sun-pointing surface, the solar pressure perturbation of a perfectly reflecting earth-pointing surface is:

1. About $\frac{1}{3}$ as large.
2. Less dependent on the initial sun angle.
3. Also characterized by small oscillations at multiples of the orbital rate.

These conclusions are predicated on the assumption of a perfectly reflecting and perfectly earth-pointing thin-plate satellite model. Perhaps the weakest aspect of the model is its implication that the along-track component of the solar radiation force does not exist. Real surfaces are bound to absorb and irradiate some incoming radiation and a non-infinitesimally-thin plate will experience along-track push of solar radiation. Although complicated satellite surface geometry and optical property make a realistic modeling difficult, perhaps a first step in the refinement of our model is to assume a certain percentage of the incoming photon tangential momentum is absorded; i.e., there exists a tangential component of the solar radiation force

$$F_r \propto \sin(\tau-\phi) \mid \cos(\tau-\phi) \mid$$

Additional refinements can also be made, although much more spohisticated modeling is probably unjustified in the presence of uncertainties in the satellite surface geometry and optical property.

As long as the solar radiation force on the satellite may be considered periodic from one orbit to another, the Fourier series method may be used to determine the orbital perturbations. As discussed before, the primary perturbations would come from force components at the orbital frequency and any constant along-track comonent.

III. EFFECT OF GM UNCERTAINTY ON TDRS ORBITS

On account of spherical symmetry, uncertainty in GM is quivalent to the following set of perturbative forces:

$$f_\theta = f_z = o, \quad f_\rho = R\,\frac{\delta GM}{GM}, \quad \left(\frac{\delta GM}{GM} = \text{fractional GM uncertainty}\right)$$

Accordingly Eq. (2) and (3) admit the following solution representing perturbations due to uncertainties in our knowledge of GM

$$\begin{bmatrix} \delta\rho(\tau) \\ \dot{\delta\rho}(\tau) \\ R\delta\theta(\tau) \\ R\dot{\delta\theta}(\tau) \end{bmatrix} = \frac{\delta GM}{GM} \begin{bmatrix} -R(1-\cos\tau) \\ -R\sin\tau \\ 2R(\tau-\sin\tau) \\ 2R(1-\cos\tau) \end{bmatrix} \tag{10}$$

The homogeneous part of the solution representing the free motion is of course still described by the matrix [A] in Eq. (5). It is seen from Eq. (10) that in addition to sinusoidal oscillations of the radial and along-track motion at the orbital rate, there is also an along-track position deviation which increases linearly with time.

The effect of GM uncertainty may be easily explained. At an orbital radius and with a circular velocity that corresponds to a slightly erroneous GM, the actual orbit is slightly elliptical with a slightly different orbital period. This is reflected in a sinusoidal variation in the radial motion plus an along-track position deviation which not only oscillates but also increases linearly with time. As expected, GM uncertainty does not cause cross-track perturbations or changes in orbital inclinations.

IV. LIMITS IN ORBIT DETERMINATION ACCURACY IN THE PRESENCE OF MODELING ERRORS

The perturbation of TDRS orbits resulting from uncertainties in our knowledge of the solar radiation force and GM was studied in the preceding sections. These perturbations represent prediction errors in the absence of tracking measurements. Measurements generally temper, but may occasionally aggravate, these errors. The ways and the extent that tracking and orbit determination strategy affect orbit accuracies in the presence of modeling errors are studied in this and the following sections.

It is usual to represent a satellite orbit by six epochal orbital elements, which, together with the dynamic model, generate a fictitious trajectory over some time span of interest. It is the role of orbit determination to pick these orbital elements such that the fictitious trajectory fits tracking measurements in some way. Thus orbit determination, as it is commonly practiced, is in essence a representation or approximation problem: i.e., seeking the representation of a real-world trajectory by a fictitious trajectory generated by six epochal elements which are to be determined. The fictitius trajectory governed by the imperfect model has a particular time characteristic which may be entirely different from that of a real-world trajectory. For instance, it maybe seen from Eq. (4) through (7) in Section II that the "real-world trajectory in the presence of solar radiation has a diverging sinusoidal variation, while a fictitious trajectory neglecting solar radiation is characterized by a linear time variation modulated by constant-amplitude sinusoidal variations. Unless the time characteristics are similar, it is obviously impossible to determine a set of <u>six</u> orbital elements which fit <u>hundreds</u> of measurement data perfectly. Thus there is an inherent limit to "orbit determination accuracy" in the presence of modeling errors.

For precision orbit determination which we are concerned with, the trajectories may be represented by small deviations from some nominal trajectory. The "true" and the "fictitions" trajectory deviations may be expressed as

$$[\delta x(t)] = \sum_i \alpha_i \, [G_i(t)] \tag{11}$$

and

$$[\Delta x(t)] = [\phi(t,t_o)][\Delta x(t_o)] \tag{12}$$

respectively. In Eq. (11) α_i represent the uncertain parameters in the model and $[G_i(t)]$ characterizes the time history of the trajectory perturbations caused by the uncertainties. The expression $[\phi(t,t_o)]$ in Eq. (12) is the state transition matrix of our imperfect trajectory model and $[\Delta x(t_o)]$ are epochal orbital elements.* The state transition matrix $[\phi(t,t_o)]$ and the trajectory perturbation matrix $[G_i(t)]$ may be readily computed from any error analysis or orbit determination program. Section II and III illustrate the simpler situation where analytical expressions for these matrices may be found.

Ideally the orbital elements $[\Delta x(t_o)]$ should be chosen such that some measure of the trajectory error ($[\delta x(t)-[\Delta x(t)]$) is minimized. A reasonable and convenient measure may be taken to be the weighted mean-square trajectory error defined as

*For simplicity we use the term orbital elements and their deviations interchangeably.

$$\frac{1}{T}\int_o^T ([\delta x(t)]-[\Delta x(t)]^T[W(t)]([\delta x(t)]-[\Delta x(t)])dt$$

$$= \frac{1}{T}\int_o^T ([\delta x(t)]-[\phi(t,t_o)](\Delta x(t_o)])^T[W(t)] \qquad (13)$$

$$([\delta x(t)]-[\phi(t,t_o)]\,[x(t_o)])dt$$

$$= [\Delta x(t_o)]^T[P][\Delta x(t_o)]-2[\Delta x(t_o)]^T[Q]+[R]$$

$$= ([\Delta x(t_o)]-[P]^{-1}[Q])^T[P]([\Delta x(t_o)]-[P]^{-1}[Q])$$

$$- [Q]^T[P]^{-1}[Q]+[R]$$

where

$$[P] \triangleq \frac{1}{T}\int_o^T ([\phi(t,t_o)]^T[W(t)][\phi(t,t_o)])dt$$

$$[Q] \triangleq \frac{1}{T}\int_o^T ([\phi(t,t_o)]^T[W(t)][\delta x(t)])dt$$

$$[R] \triangleq \frac{1}{T}\int_o^T ([\delta x(t)]^T[W(t)][\delta x(t)])dt$$

$[W(t)] \triangleq$ a non-negative weighting matrix

Since [P] is positive-definite, it is obvious from Eq. (13) that the mean-square trajectory error has the minimum value

$$[R]-[Q]^T[P]^{-1}[Q] \tag{14}$$

which is achieved if the epochal orbital elements are taken as

$$[\Delta x(t_o)]=[P]^{-1}[Q]$$

$$=\left\{\int_o^T ([\phi(t,t_o)^T[W(t)][\phi(t,t_o)]dt\right\}^{-1} \tag{15}$$

$$\sum_i \alpha_i \int_o^T [\phi(t,t_o)]^T[W(t)][G_i(t)]dt$$

The corresponding trajectory error in time becomes

$$[\delta x(t)]-[\phi(t,t_o)][\Delta x(t_o)] \tag{16}$$

$$=\sum_i \alpha_i \left([G_i(t)]-[\phi(t,t_o)]\left\{\int_o^T [\phi(t,t_o)]^T[W(t)]\right.\right.$$

$$\left.\left.[\phi(t,t_o)]dt\right\}^{-1}\int_o^T [\phi(t,t_o)^T[W(t)][G_i(t)]dt\right)$$

obviously the trajectory error vanishes if

$$\sum_i \alpha_i \, [G_i(t)] = [\phi(t,t_o)][K],$$

i.e., if the time characteristics of the actual trajectory perturbations are similar to these of the fictitious trajectory. As mentioned above, the trajectory perturbation matrices $[G_i(t)]$ and the state transition matrix $[\phi(t,t_o)]$ are readily avaibable from most orbit error analysis programs. Thus, once the expected levels of model uncertainties α_i are specified, Eq. (13) and (16) may be readily integrated to give the time history of the expected limiting orbital accuracy as well as the minimum weighted mean-square trajectory error.

Although not a prescription for the optimum tracking and orbit determination strategy, the limiting accuracy thus computed plays a very useful role, i.e., as a yardstick for measuring the performance of any tracking and orbit determination strategy. Once a particular tracking and orbit determination procedure is proposed, the expected trajectory error may be computed from an orbital error analysis program such as ORAN (Ref. 7). A comparison of this error with the limiting accuracy tells us whether that particular strategy is already close to the optimum, or whether there is considerable room for improvement and other strategies should be tried.

To illustrate the result of this section we shall make use of the state-transition matrix and the solar radiation perturbation matrix derived in Section II to study the limiting orbital accuracy in the presence of uncertainties in solar radiation pressure. In essence, solar radiation perturbation appear as diverging sinusoids $\tau\sin\tau$ (sun overhead initially) and $\tau\cos\tau$ (sun behind velocity vector initially). The orbit

determination process may compensate for this perturbation by linear variations in time plus simple sinusoids, i.e., $\alpha+\beta\tau+\gamma\sin\tau+\delta\cos\tau$. The optimum approximations are shown in Fig. 4 and 5 and indicate the approximation for $\tau\cos\tau$ is quite good while that for $\tau\sin\tau$ is less satisfactory. One sees that, ideally, with tracking and orbit determination, it may be possible to reduce the along-track orbital error to approximately $0.512/2\pi \approx 0.08$ of its maximum perturbations for the case when the sun is initially over-head. On the other hand, for the case when the sun is initially behind the satellite velocity vector, tracking and orbit determination is much less effective, and can only reduce the along-track error to approximately $1.5/(3\pi/2) \approx 0.3$ of its maximum perturbations. This is the explanation for the seemingly perplexing phenomenan that although perturbations caused by solar radiation are much more serious starting from the position when the sun is directly over-head, yet the use of tracking may reduce the error considerable so that the orbit determination error may only be one-third as large as the corresponding error starting from the epoch that the sun is behind the satellite velocity vector. The latter case was shown to be comparatively less sensitive to solar radiation perturbations in the absence of tracking.

V. INFORMATION CONVEYED BY RANGE MEASUREMENTS AND VARIATION OF TDRS ORBITAL ERROR WITH TRACKING BASELINE

Since the modeling uncertainties are unknown, it is not possible to compute the optimum orbital elements according to Eq. (15) in the preceeding section. In practice, the orbital elements are computed such that the resulting fictitious trajectory fits the measurements. Different kinds of measurements convey information about different aspects of the trajectory. If the measurements contain more information about

the orbital height, then the computed orbit would tend to fit the correct height at the expense of, say, along-track accuracies. Thus it is important to know the information content of the measurements in order to understand orbit determination accuracies in the presence of modeling errors.

Tracking of TDRS consist of bilateration from two ground stations (Fig. 6). Expressed in terms of deviations from the nominal, the range measurements may be written as

$$\delta\rho_1 = \vec{\delta R} \cdot \vec{i}_1$$

$$\delta\rho_2 = \vec{\delta R} \cdot \vec{i}_2$$

where $\vec{\delta}_R$ is the satellite position deviation and the $\vec{i}$'s are unit vectors in station-to-TDRS directions. One may consider these equations as describing the resolution of the unknown position deviation $\vec{\delta R}$ along the directions defined by the unit vectors $\vec{i}_1$ and $\vec{i}_2$. For the high altitude TDRS, these are close to the orbital radius direction. In other words, individial measurements convey mostly orbital height information Along-track and cross-track information is contained in an equation obtainable by multiplying the above equations by the range ρ_1 and ρ_2 respectively and then subtracting one from the other, i.e.,

$$\rho_1\delta\rho_1 - \rho_2\delta\rho_2 = \vec{\delta R}\cdot(\vec{\rho}_1 - \vec{\rho}_2) = \vec{\delta R}\cdot(\vec{r}_1 - \vec{r}_2),$$

where $(\vec{r}_1 - \vec{r}_2)$ is the tracking baseline, i.e., the vector connecting the two tracking stations. To increase the sensitivity and therefore the information content one should select the tracking stations such that

1. $|\vec{r}_1 - \vec{r}_2|$ is as large as possible.

2. $\vec{r}_1 - \vec{r}_2$ should have a large component in the important along-track direction. However it should also have some component in the cross-track direction to sense cross-track errors.

Error analysis results on TDRS orbital accuracy for a series of different ground transponder locations are given in Ref. 2. The central ground terminal is considered fixed at White Sands, New Mexico (254° Longitude, 32° Latitude). Tracking baseline geometry changes with ground transponder location which varies at certain increments of longitude and latitude. To bring out the connection between orbital errors and bilateration baseline, the orbital errors given in Ref. 2 were correlalated with parameters defining the tracking baseline such as the baseline great circle length and inclination, along-track and cross-track baseline length, and latitude and longitude separation of the two stations. Representative results showing the close correlation between the along-track and cross-track orbital errors and the corresponding tracking baseline components are presented in Table 1 and Fig. 7, from which the following information may be extracted:

1. For the error model considered, orbital errors vary from approximately 110 meters to 350 meters. The latter occurs when the transponder location is unfavorable.

2. There is good correlation between cross-track orbital error and the component of tracking baseline in the cross-track direction. When the cross-track error is less than 50 meters, it has a negligible contribution to the RSS total error. In general this requires the tracking baseline to have a component in the cross-track direction greater than 0.7 of the earth's radius.

3. There is also good correlation between along-track orbital error and the component of tracking baseline in the along track direction. To limit the along-track error below 140 meters, a baseline component length of 1.2 earth radius is required. A baseline component lenght of 1.5 earth radius is required to keep the along-track error under 120 meters.

4. Since the TDRS's considered have 7° inclination, they are not quite geo-stationary. The along-track and cross-track components of the bilateration baseline used in the preceeding paragraphs are somewhat arbitrarily computed assuming the TDRS's are at the ascending node. More convenient but less precise characterizations of the along-track and cross-track baseline components are the longitude and latitude separations of the two stations. For the central terminal fixed at 254° Longitude and 32° Latitude, the transponder should preferably be located in the southern hemisphere with a longitude separation as large as practicable.

VI. RANGE-RATE MEASUREMENTS AND INSENSITIVITY OF RANGE-RATE ORBIT SOLUTIONS TO GM ERROR

The range-rate from a tracking station to a satellite may be expressed as

$$\dot{\rho}=\vec{v}\cdot\vec{i}_{\rho}$$

where $\vec{v}$ is the velocity of the satellite relative to the rotating earth. Thus the deviations are,

$$\delta\dot{\rho}=\vec{v}\cdot\delta\vec{i}_{\rho}+\delta\vec{v}\cdot\vec{i}_{\rho}$$

The unit vector i_ρ is close to the radial direction. δi_ρ is orthogonal to $\vec{i}_\rho$ and is primarily the result of the along-track and cross-track position deviations. Thus the range-rate measurement convey radial velocity information together with some positional information. For the geosynchronous TDRS $\vec{v}$ is primarily in the cross-track direction. Thus the along-track positional information content is weak in the range-rate measurements.

Since the TDRS is nearly geo-stationary, range tracking contains much more information than range-rate tracking, and the TDRS orbits are computed essentially from range measurements. However it is known from error analysis studies that orbits of TDRS or other high altitude satellites such as the GPS spacecraft are much less sensitive to GM errors if the orbit solutions are based on range-rate rather than range trackings. This may be explained as follows. It was shown in Section III that GM uncertainty causes a perturbation which as the following time characteristics

$$\begin{bmatrix} \text{Height} \\ \text{Radial Velocity} \\ \text{Along-Track Position} \end{bmatrix} \propto \begin{bmatrix} \cos\tau - 1 \\ -\sin\tau \\ 2(\tau - \sin\tau) \end{bmatrix}$$

On the other hand, trajectory error propagated from initial height error has the following characteristics

$$\begin{bmatrix} \text{Height} \\ \text{Radial Velocity} \\ \text{Along-Track Position} \end{bmatrix} \propto \begin{bmatrix} \frac{4}{3} - \cos\tau \\ \sin\tau \\ 2(\sin\tau - \tau) \end{bmatrix}$$

Since range-rate measurements convey mostly radial velocity information, the computed orbit tends to fit the radial velocity perturbation by attributing it to an initial height deviations. The above equations show this also gives a correct along-track position while there would be a constant height error. Indeed this is what error analysis result tells us. Physically this is also obvious. With a correct orbital period, an incorrect GM would result in an incorrect semi-major axis or height. On the other hand, an orbital solution based on range tracking would tend to fit the height and as the above equations show, must result in along track errors. Along-track errors are usually larger than height errors, thus range tracking orbital solutions are more susceptible to GM errors.

In general, perturbation due to GM uncertainty has a time characteristic quite similar to the time characteristic of a trajectory propagated from some initial conditions. Thus tracking can compensate for GM uncertainty much more than, say the solar radiation uncertainty.

VII. ORBIT DETERMINATION ERROR CHARACTERISTICS

Much of the orbit determination error characteristics may be illustrated or explained based on the simplified orbit model derived in Section II. It is shown there that by adjusting the epochal elements $[\delta\rho(0)\ \dot{\delta\rho}(0)\ R\delta\theta(0)\ R\dot{\delta\theta}(0)]$, trajectory deviations of the following form may be obtained.

$$\begin{bmatrix} \delta o(\tau) \\ \dot{\delta\rho}(\tau) \\ R\delta\theta(\tau) \\ R\dot{\delta\theta}(\tau) \end{bmatrix} = \begin{bmatrix} 4-3\cos\tau & \sin\tau & 0 & 2(1-\cos\tau) \\ 3\sin\tau & \cos\tau & 0 & 2\sin\tau \\ 6(\sin\tau-\tau) & 2(\cos\tau-1) & 1 & 4\sin\tau-3\tau \\ 6(\cos\tau-1) & -2\sin\tau & 0 & 4\cos\tau-3 \end{bmatrix} \begin{bmatrix} \delta\rho(0) \\ \dot{\delta\rho}(0) \\ R\delta\theta(0) \\ R\dot{\delta\theta}(0) \end{bmatrix}$$

The following characteristics of the trajectory time history as described by the above equations may be emphasized:

1. Along-track position may have constant deviations, linear growth, as well as sinusoidal variations at orbital frequency.

2. Other orbital position and velocity deviations may exhibit constant biases plus sinusoidal variations at orbital frequency.

3. The trajectory may be shifted by a constant amount in along-track position without affecting other aspects of the trajectory.

In contrast, "real perturbations", governed by the equations of motion (2a) and (3a), may consist of linearly diverging oscillations, constant amplitude high frequency oscillations, as well as linear and quadratic growth in the along-track position. Thus orbits computed cannot account for the high frequency components, nor any secular growth in the orbital height, nor any diverging oscillations or any "super-linear" growth in along track position.

- Large Errors Near Beginning And End of Tracking Arc, Oscillatory Behavior of Orbital Errors, and Deterioration of Accuracy With Length of Tracking Arc

The phenomena described by the above statement are frequently observed in the course of orbital error analysis studies. The explanation for the occurrence of these phenomena is almost obvious from the preceding discussions. Generally, along-track orbital errors are the most serious, as any perturbations in orbital rate will propagate into large along-track position errors. Fig. 8 illustrates that the along-track position

perturbations generally consist of "super-linear" growth with diverging oscillations at the orbital rate together with possible constant-amplitude high frequency oscillations characteristics of some perturbation forces. On the other hand, computed orbits tend to approximate this perturbation by linear gorwths plus constant amplitude sinusoidal oscillations (not shown) at the orbital rate. Line A represents perhaps the best approximation one may hope for. Line B and C represent progressively worse orbits. In any case, orbital accuracies are going to deteriorate as tracking arc lenghtens. If tracking measurements convey along-track position information, most commonly one has the situation represented by the line B, which is characterized by larger and opposite errors at the beginning and the end of the tracking arc, and reduced errors in the middle. It is also obvious that high frequency excitations contained in the perturbative force will persist as high frequency orbital errors although the amplitudes may be somewhat attenuated because, as shown before, the satellite radial motion behaves as a simple harmonic oscillator tuned at the orbital frequency and that there exists coupling between the radial and along-track motions.

The above theory has since been validated and found fruitful applications in the study of the effect of drag on low altitude satellite orbit determination (Ref. 8).

VIII. REFERENCES

1. Fang, B.T., and Gibbs, B.P., "TDRSS Era Orbit Determination Review Study," Planetary Sciences Department Report No. MT010-75, Wolf Research and Development Group, EG&G Washington Analytical Services Center, Inc., December 1975.

2. Campion, R.E., "TDRS Error Analysis," Tracking Data Evaluation Office, Bendix Corp., October 17, 1977.

3. Shrivastava, S.K., "Orbital Perturbations and Station Keeping of Communication Satellites," J. of Spacecraft, March-April, 1978.

4. Fang, B.T., "Short-Term Solar Pressure Effect and GM Uncertainty on TDRS Orbital Accuracy - A Study of the Interaction of Modeling Error With Tracking and Orbit Determination," Applied Systems Department Report No. 002-78, EG&G Washington Analytical Services Center, Inc., October, 1978.

5. Geyling, F.T., and Westerman, H.R., "Introduction to Orbital Mechanics," Addison Wesley, Reading, Mass.. 1971.

6. Fang, B.T., and Brown, J.H., "Orbital Guidance and Rendezvous Using Perturbation Method," AIAA Paper No. 67-55, January 1967.

7. Hatch, W., and Goad, C., "Mathematical Description of the ORAN Error Analysis Program," Wolf Research and Development Corporation Report No. 009-23, August 1973.

8. Fang, B.T., "Orbit Determination and Navigation Studies (TDRSS/GPS)" Applied Systems Department Report No. 004-78, EG&G Washington Analytical Services Center, Inc. November 1978.

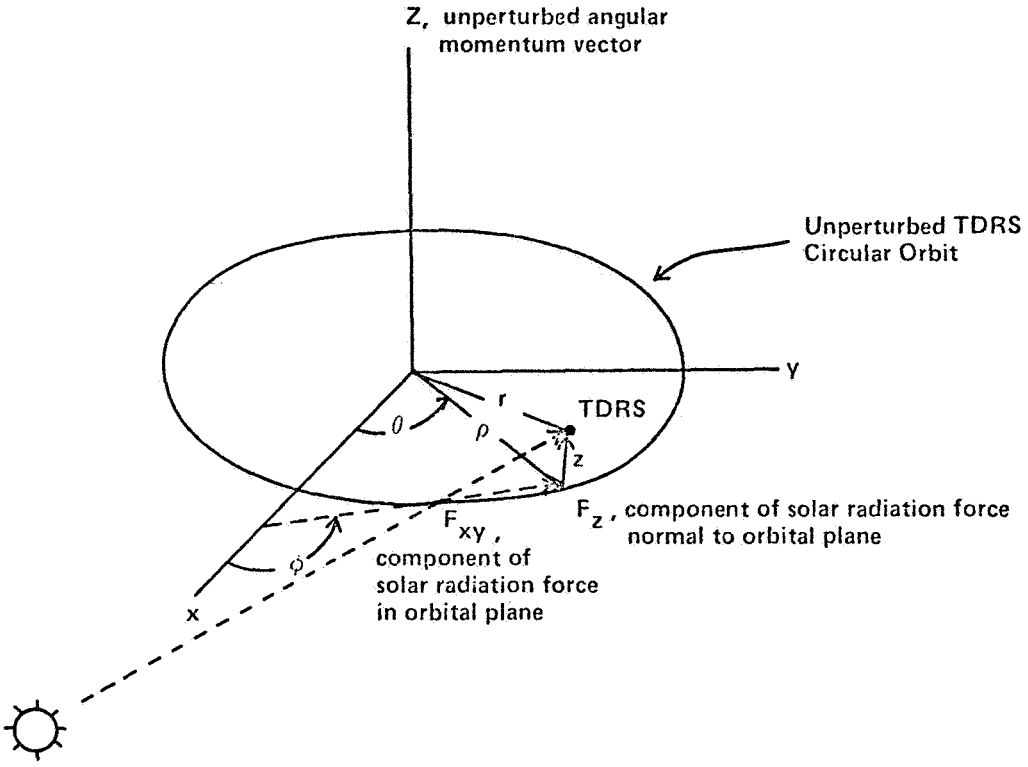

FIGURE 1. COORDINATE AXES AND RELATIVE GEOMETRY OF TDRS AND SUN

f_{xy} = component of solar radiation force (normalized) in TDRS orbital plane

ϕ = angle between f_{xy} and orbital radius vector at $\tau = 0$

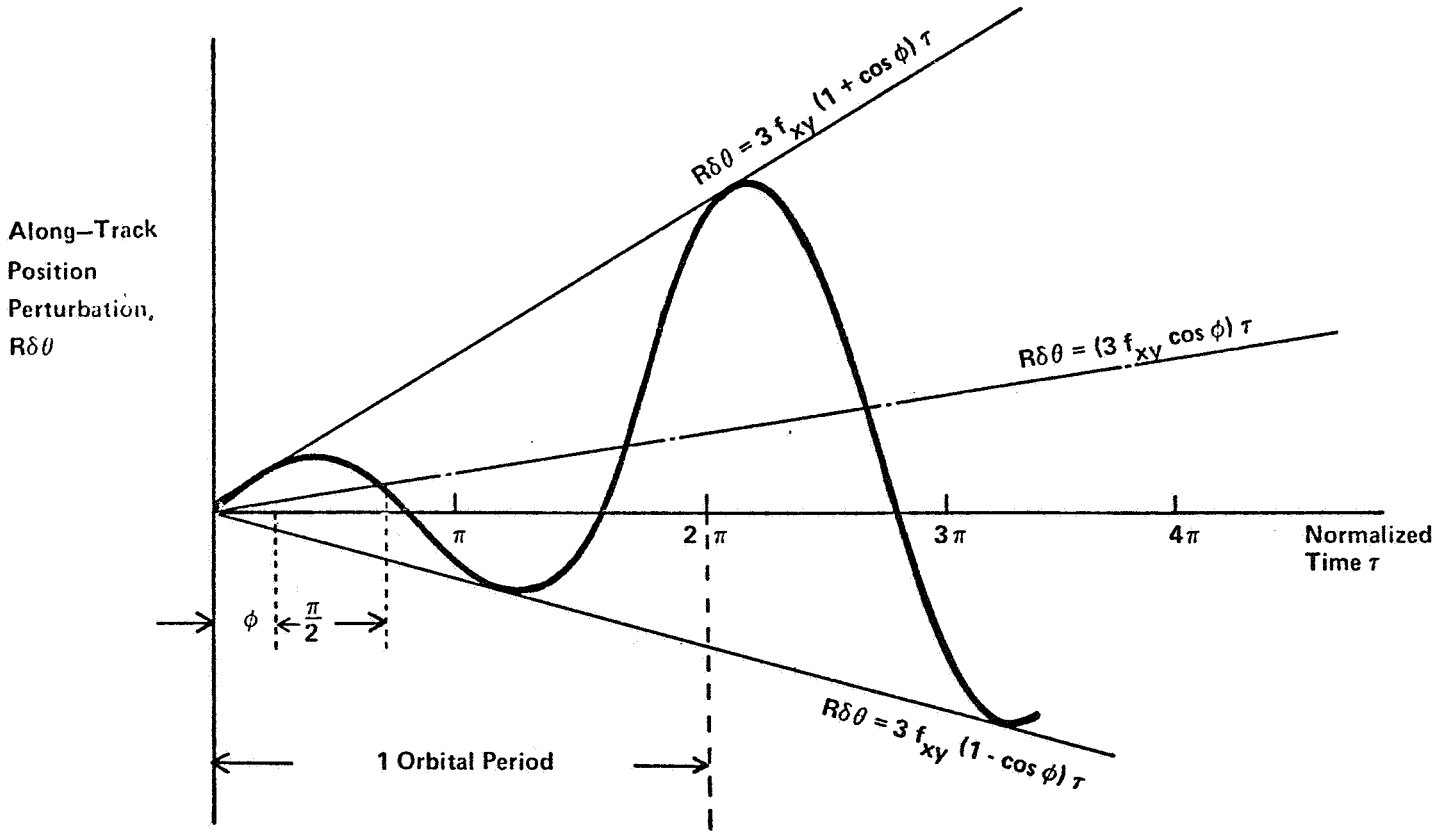

FIGURE 2. VARIATIONS OF ALONG–TRACK ORBITAL POSITION PERTURBATION Rδθ WITH NORMALIZED TIME τ AND INITIAL SUN ANGLE ϕ

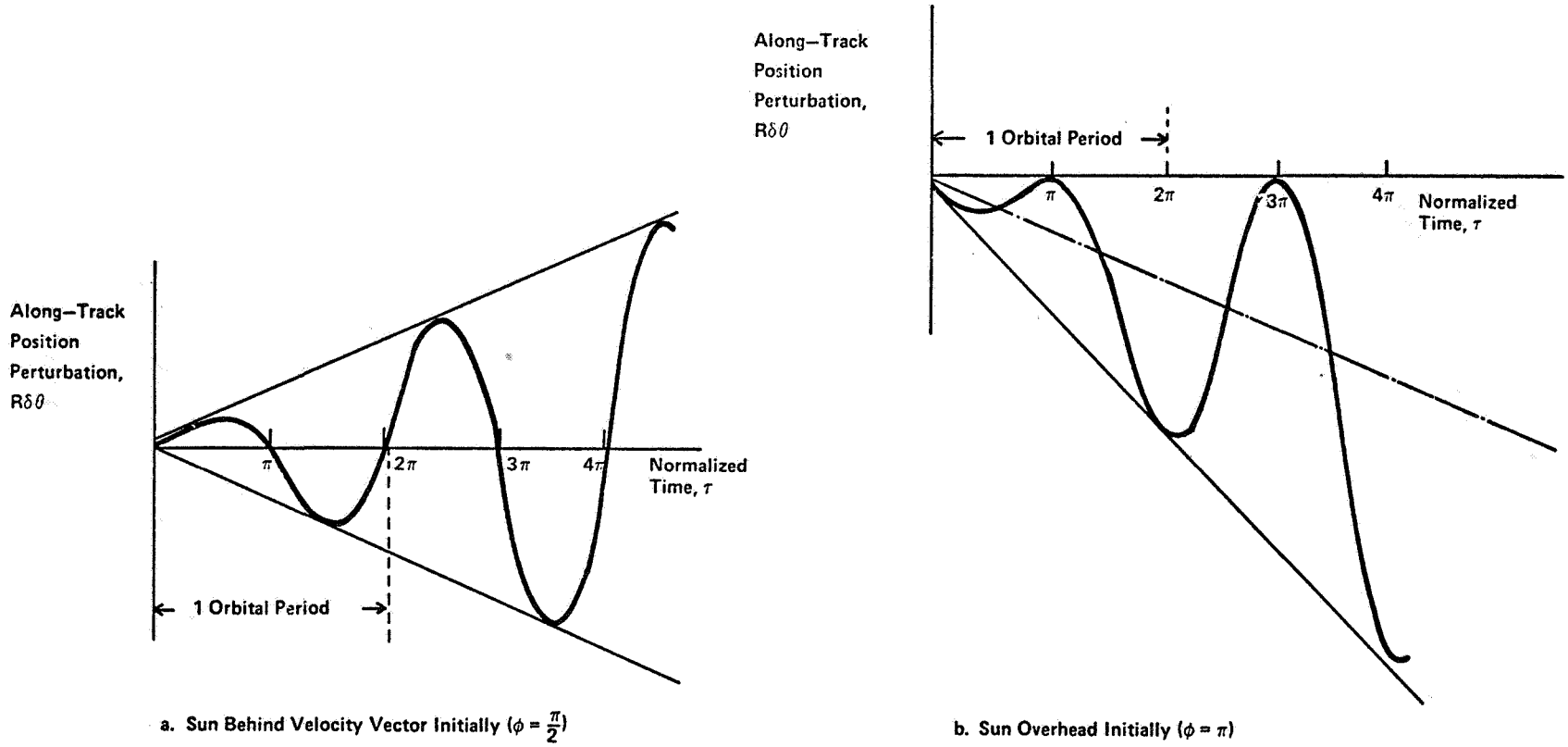

a. Sun Behind Velocity Vector Initially ($\phi = \frac{\pi}{2}$)

b. Sun Overhead Initially ($\phi = \pi$)

FIGURE 3. ALONG TRACK POSITION PERTURBATION CAUSED BY SOLAR RADIATION PRESSURE

FIGURE 4. DIVERGING SINUSOID $\tau \sin \tau$ AND THE APPROXIMATION BY $\pi \sin \tau - \frac{1}{2} \cos \tau - 1$

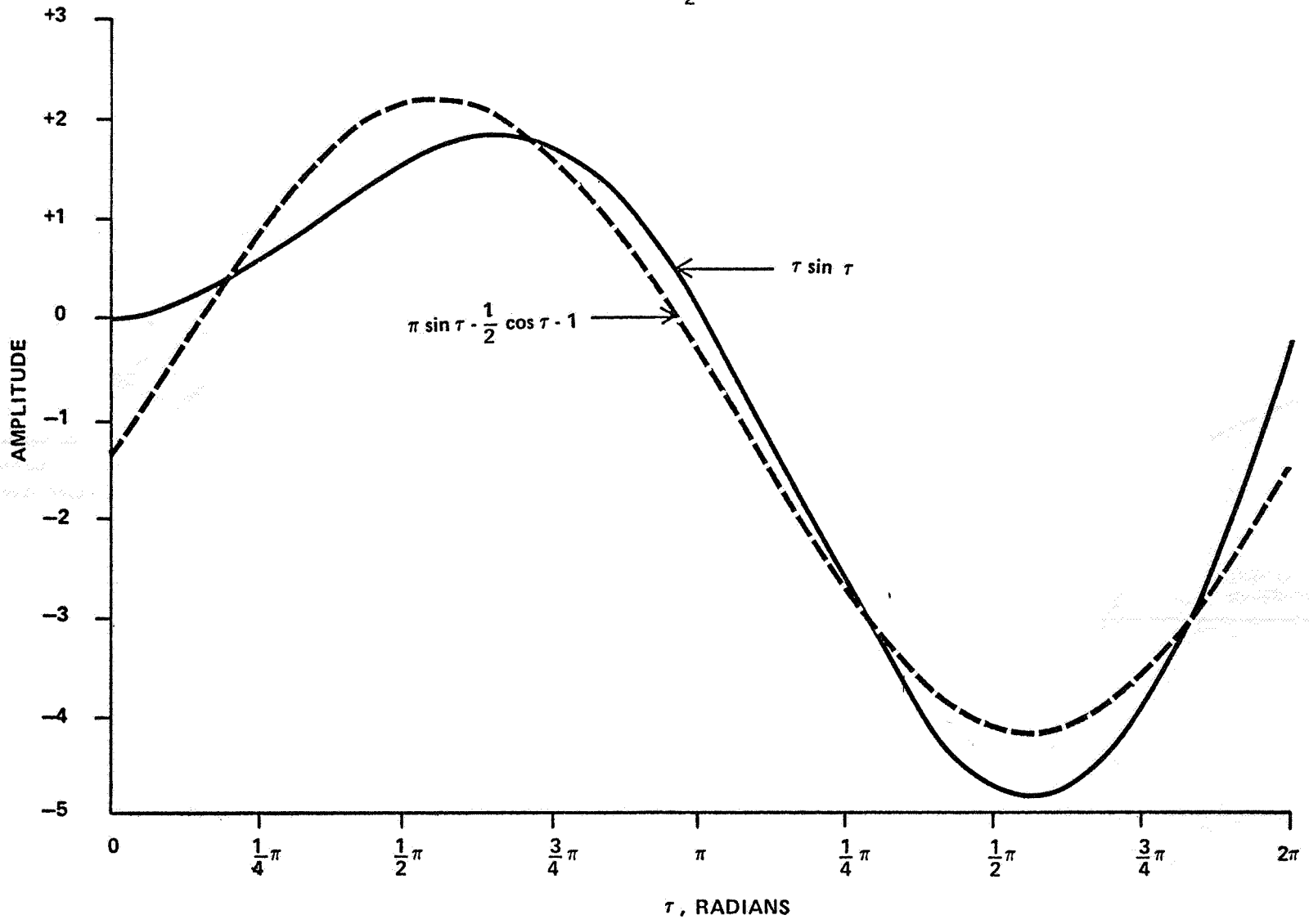

FIGURE 5. DIVERGING SINUSOID $\tau \cos \tau$ AND APPROXIMATIONS BY
$\pi \cos \tau + 1.8258 \sin \tau + 1.1634 \tau - 3.6534$

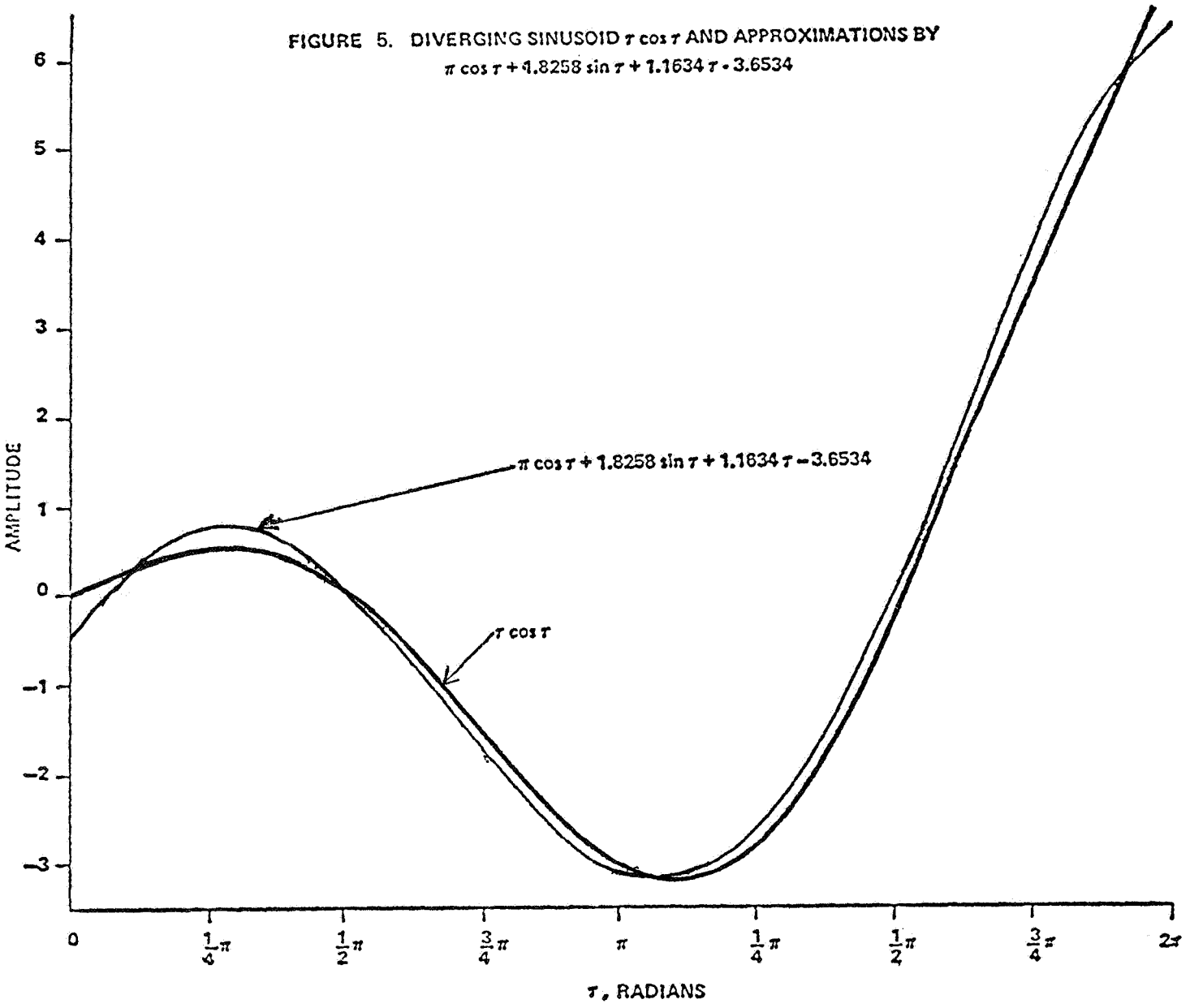

FIGURE 6. INFORMATION CONTENT OF RANGE MEASUREMENTS

INDIVIDUAL MEASUREMENTS GIVE HEIGHT INFORMATION

$$\delta\rho_1 = \delta\bar{R} \cdot \bar{i}_1$$

$$\delta\rho_2 = \delta\bar{R} \cdot \bar{i}_2$$

BILATERATION GIVES INFORMATION ALONG TRACKING BASELINE

$$\rho_1 \delta\rho_1 - \rho_2 \delta\rho_2 = \delta\bar{R} \cdot \underline{(\bar{r}_1 - \bar{r}_2)}$$

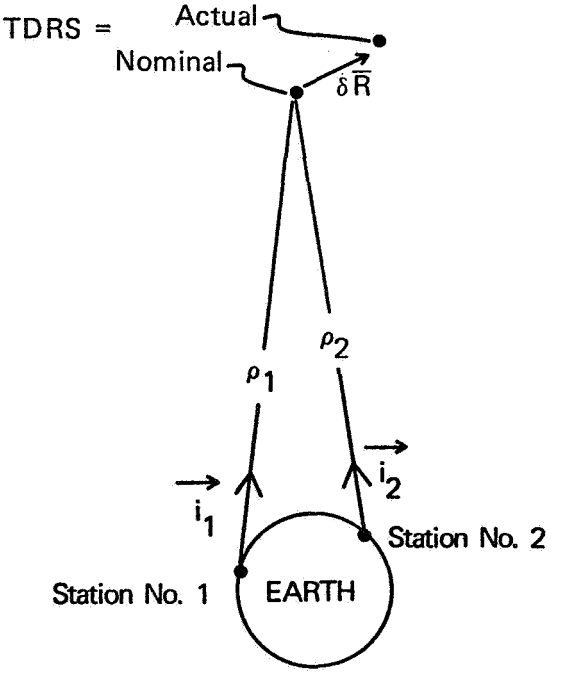

FIGURE 7. TDRS–W ALONG–TRACK POSITION ERROR VS. BILATERATION BASELINE ALONG–TRACK COMPONENT

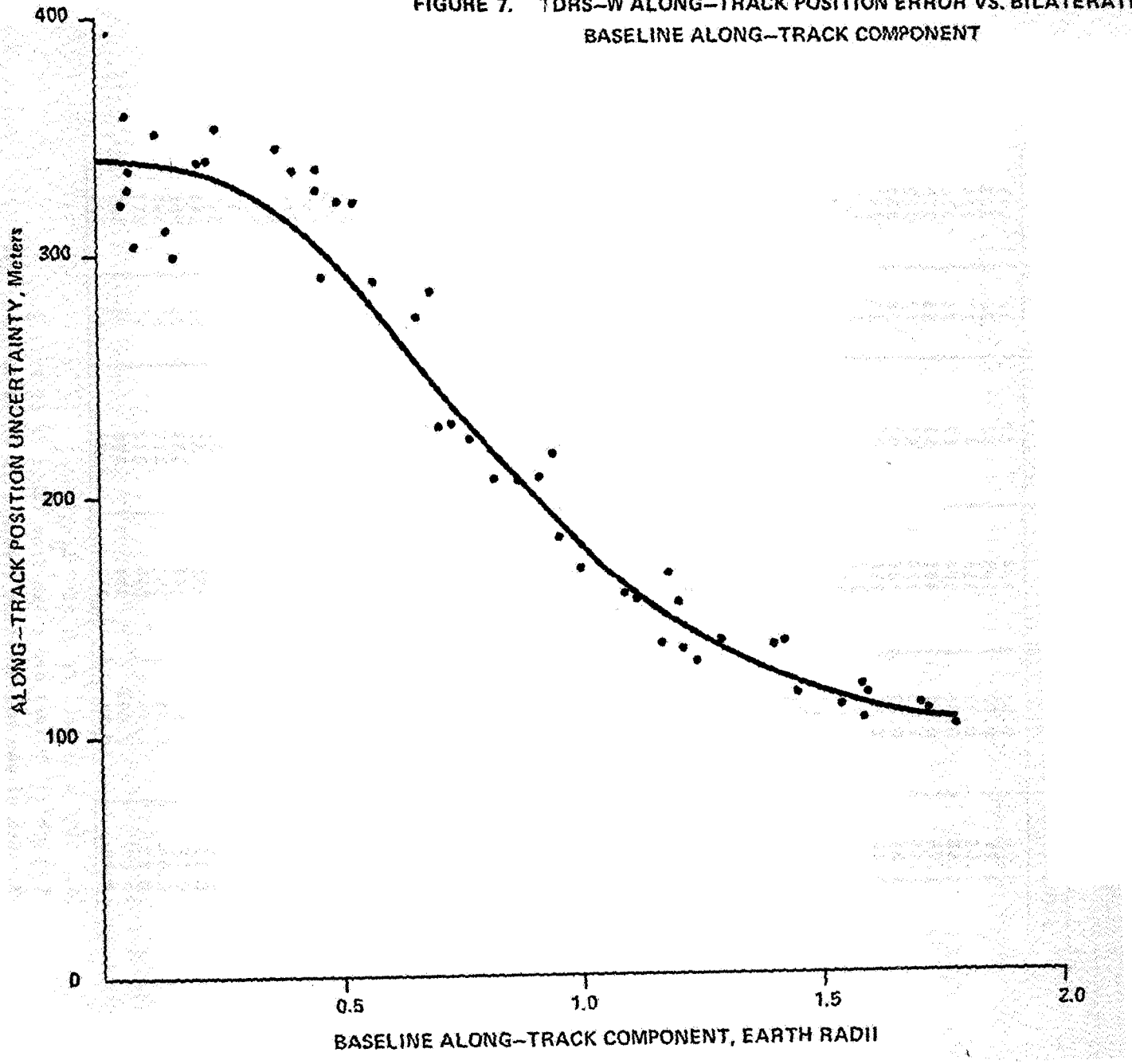

Table 1. Correlation of TDRS-W Orbital Error With Bilateration Baseline Geometry

BILATERATION BASELINE COMPONENT (earth rad.)		ORBITAL ERROR (m.)			
ALONG-TRACK	CROSS-TRACK	ALONG-TRACK	CROSS-TRACK	RADIAL	RSS TOTAL
1.78	0.58	104	67	16	111
1.71	0.82	109	51	16	113
1.53	0.71	111	49	17	115
1.58	0.35	104	81	16	116
1.78	0.32	103	91	15	122
1.58	1.03	119	41	17	122
1.24	0.39	128	64	18	134
1.40	1.21	136	35	18	139
1.29	1.04	137	32	19	139
1.21	0.57	135	47	19	139
1.17	0.22	136	88	18	147
1.71	0.68	108	132	18	159
1.09	0.77	168	35	21	161
1.44	0.00	115	138	18	166
1.18	1.33	165	34	21	169
1.20	0.45	154	96	20	178
1.13	0.26	155	105	22	179
1.42	0.32	136	124	20	184
1.00	0.06	168	122	21	188
1.59	0.15	115	166	22	192
0.96	0.52	181	108	21	205
0.87	0.86	205	32	25	208
0.82	0.44	205	38	25	209
0.92	1.20	206	30	25	209
0.94	1.40	215	37	26	219
0.73	0.32	227	95	28	237
0.77	0.02	222	129	27	241
0.71	0.52	226	106	24	245
0.66	0.82	273	35	31	275
0.69	1.40	283	41	32	287
0.57	0.11	287	109	31	303
0.14	0.56	298	42	36	304
0.07	0.81	303	30	37	307
0.46	0.58	289	114	30	308
0.53	1.14	319	36	36	321
0.50	0.65	320	37	35	323
0.05	1.02	320	32	38	323
0.14	0.30	309	100	35	326
0.06	0.53	326	42	37	331
0.40	0.50	325	63	34	333
0.45	1.33	333	37	37	335
0.40	0.49	333	42	36	337
0.21	0.87	337	32	39	340
0.23	1.20	338	32	39	341
0.37	0.17	343	138	38	361
0.24	0.34	351	118	37	368
0.12	0.16	350	142	37	377
0.07	0.06	334	198	39	385
0.06	0.16	357	184	40	396

1. TDRS-W is located at 189° Longitude.
2. Orbital errors are taken from Table 38 of Ref. 2.
3. One of the bilateration stations is White Sands at 254° Longitude and 32° Latitude. The other station (transponder) location varies, giving rise to different baseline geometry.